Combustion and Flame xxx (2013) xxx–xxx

Contents lists available at SciVerse ScienceDirect

Combustion and Flame

journal homepage: www.elsevier.com/locate/combustflame

Flame propagation in a tube with wall quenching of radicals

Bin Bai [a], Zheng Chen [a,b,c,*], Huangwei Zhang [a,1], Shiyi Chen [a,c]

[a] SKLTCS, Department of Mechanics and Aerospace Engineering, College of Engineering, Peking University, Beijing 100871, China
[b] SKLTCS, Department of Aeronautics and Astronautics, College of Engineering, Peking University, Beijing 100871, China
[c] Center for Computational Science and Engineering, Peking University, Beijing 100871, China

ARTICLE INFO

Article history:
Received 31 January 2013
Received in revised form 3 July 2013
Accepted 3 July 2013
Available online xxxx

Keywords:
Flame propagation in a tube
Radical quenching
Heat loss
Extinction limit

ABSTRACT

In micro- and meso-scale combustion, there exists strong flame-wall interaction and flame can be quenched by thermal and kinetic mechanisms. The thermal quenching mechanism has been well studied while the kinetic quenching mechanism has received little attention. To provide an incremental advance to former analytical models, we conduct theoretical analysis on flame propagation in a tube with emphasis on both thermal and kinetic quenching mechanisms. A two-step chemistry model for gaseous combustion is employed and it consists of a chain-branching reaction and a completion reaction. To mimic the wall quenching of radicals, a one-step surface quenching reaction of radicals is considered. A general theoretical description of quasi-one-dimensional flame propagation in a tube with both heat loss and radical quenching is presented. An analytical correlation, which describes the change of the flame propagation speed with heat loss and radical quenching coefficients, is derived. Based on this correlation, the effects of radical Lewis number, cross-over temperature, wall temperature, and tube diameter on flame speed and quenching limit are examined. The results show that the impacts of both heat loss and radical quenching become stronger at smaller radical Lewis number. With the increase of cross-over temperature, flame extinction due to heat loss and that due to radical quenching are shown to be promoted and inhibited, respectively. With the increase of wall temperature, both the thermal and kinetic quenching limits are significantly extended. With the decrease of the tube diameter, flame extinction occurs due to thermal and/or kinetic quenching. It is found that the radical quenching effect becomes stronger at higher wall temperature and/or lower cross-over temperature.

1. Introduction

To develop high-specific-energy micro-electro-mechanical power systems, stable and complete combustion at small scales (micro and mesoscales) should be realized. However, with the reduction in combustor's length scale, the surface-to-volume ratio increases and the wall effects become crucial in flame propagation and extinction. In fact, at large surface-to-volume ratio, there is strong flame-wall interaction and the flame can be quenched by thermal and kinetic mechanisms [1–4]. The thermal mechanism refers to heat loss to the wall and the kinetic mechanism refers to radical quenching on wall surface [2–4]. Both mechanisms play important roles in small scale combustion, especially for flame near the extinction limit [1–4].

The thermal quenching mechanism is well known. Previous studies have demonstrated that there exists a quenching tube diameter (or channel distance) below which flame cannot propagate [5,6]. Recently, the flame-wall thermal coupling has been extensively studied and the influence of heat recirculation [7] on flame propagation in small scale combustor has been systematically examined [8–20]. It has been found that the flammability limit and quenching diameter can be greatly extended through heat recirculation and that there exist different flame regimes/patterns/bifurcations due to flame-wall thermal coupling. Research process on flame-wall coupling and thermal quenching mechanism in small scale combustion has been reviewed by Ju and Maruta [2,3].

Compared to the thermal quenching mechanism, the kinetic quenching mechanism has received significantly less attention and only a few studies have been conducted to assess the radical quenching effect in small scale combustion. Popp et al. [21,22] and Aghalayam et al. [23,24] simulated the head-on quenching process of a premixed flame considering detailed gas-phase chemistry as well as surface radical completion reactions, and examined the role of wall quenching of radicals. Raimondeau et al. [25] conducted two-dimensional simulations of flame propagation in a non-adiabatic straight channel and investigated the gas-surface interfacial phenomena. Ju and Xu [26] considered four-step

* Corresponding author at: SKLTCS, Department of Mechanics and Aerospace Engineering, College of Engineering, Peking University, Beijing 100871, China.
E-mail address: cz@pku.edu.cn (Z. Chen).
[1] Current address: University of Cambridge, UK.

0010-2180/$ - see front matter © 2013 The Combustion Institute. Published by Elsevier Inc. All rights reserved.
http://dx.doi.org/10.1016/j.combustflame.2013.07.008

chemistry model (which describes the chain-initiation, branching, and termination processes as well as radical quenching on wall surface) in their simulation and examined the radical quenching limit at different wall temperatures and tube diameters. They found that radical quenching has stronger influence on flame propagation at higher wall temperature [26]. Experimentally, Miesse et al. [27] found that the quenching distance depends more strongly on wall materials at higher wall temperature. They concluded that the thermal and radical quenching is dominant at low and high wall temperature, respectively. Saiki and Suzuki [46] investigated experimentally and numerically the effects of wall materials on radical quenching in a methane–air premixed flame and provided detailed information on surface activity of four materials and their effects on the flame. Yang et al. [28] also examined experimentally the effects of wall material on flame quenching and they found that radical quenching is mainly controlled by the percentage of chemisorbed oxygen on wall surface. More recently, Wang and Law [48] have studied the explosion limits of hydrogen–oxygen mixtures and they showed that the wall destruction of radicals is crucial to the Z-shaped explosion limits.

Except the computational work of Ju and Xu [26], all the simulations and experiments mentioned above were limited to specific fuel/air mixtures and wall materials. Therefore, the general kinetic quenching mechanism is still not well understood. Theoretical analysis for flame propagation in a tube/channel with heat loss and radical quenching on the wall can provide a general understanding of the thermal and kinetic quenching mechanisms. Besides, it can possibly provide solutions of reference for code validation. Therefore, it is meaningful to develop a theoretical model for flame propagation in a tube with wall quenching of radical. However, in traditional theoretical analysis of premixed flames, one-step, irreversible, global reaction model was usually employed. In one-step chemistry model, fuel is converted directly into products and hence the role of active radicals is not included. Therefore, to the authors' knowledge, there is no theoretical analysis in the literature examining the radical quenching effect on flame propagation in a small tube/channel.

The objectives of the present study are to provide a general theoretical description of flame propagation in a tube with wall quenching of radicals and to examine the influence of different factors on thermal and kinetic quenching limits. First, we shall introduce a theoretical model for flame propagation in a tube considering thermally sensitive intermediate kinetics and surface radical quenching reaction, and derive a correlation describing the change of the flame propagation speed with heat loss and radical quenching on the wall. Then, based on this correlation, we shall assess the effects of radical Lewis number, cross-over temperature, wall temperature, and tube diameter on thermal and kinetic quenching limits.

2. Theoretical analysis

In this section, we present a general theoretical description of flame propagation in a tube with wall quenching of radicals and heat loss.

2.1. Chemical reactions

As mentioned before, one-step global reaction model cannot be used to study the radical quenching effect. As such, chain-branching kinetics of intermediate species (radicals) should be considered in theoretical analysis. We employ the two-step chain-branching model proposed by Dold and coworkers [29–31]. This model consists of a chain-branching reaction and a completion reaction:

$$\mathrm{F}+\mathrm{Z}\rightarrow 2Z,\quad \widetilde{\omega}_B=\frac{\widetilde{\rho}\widetilde{Y}_F}{\widetilde{W}_F}\frac{\widetilde{\rho}\widetilde{Y}_Z}{\widetilde{W}_Z}\widetilde{A}_B\exp\left(-\frac{\widetilde{T}_B}{\widetilde{T}}\right) \tag{1}$$

$$\mathrm{Z}+\mathrm{M}\rightarrow \mathrm{P}+\mathrm{M},\quad \widetilde{\omega}_C=\frac{\widetilde{\rho}\widetilde{Y}_Z}{\widetilde{W}_Z}\frac{\widetilde{\rho}}{\widetilde{W}}\widetilde{A}_C \tag{2}$$

where F, Z, and P denote fuel, radical, and product, respectively, and M represents any third body species. The reaction rates are given in Eqs. (1) and (2) with $\widetilde{\rho}$ being density, $\widetilde{Y}_F$ and $\widetilde{Y}_Z$ the mass fractions of fuel and radical, $\widetilde{W}_F$ and $\widetilde{W}_Z$ the molecular weights of fuel and radical, $\widetilde{W}$ the mean molecular weight, $\widetilde{A}_B$ and $\widetilde{A}_C$ the frequency factors, $\widetilde{T}_B$ the activation temperature, and $\widetilde{T}$ the temperature of the mixture. The chain-branching reaction has high activation energy and is thermally neutral, while the completion reaction is temperature insensitive (zero activation energy) and releases all the heat [31]. This two-step chain-branching model was used in previous studies on the ignition, propagation, extinction, and stability of premixed flames [29–40].

The radical loss due to surface reaction is considered in this study. The surface reaction and its reaction rate are [6]:

$$\mathrm{Z}\xrightarrow{\text{Wall}}\text{quenching},\quad \widetilde{\omega}_W=\widetilde{\gamma}_s\frac{1}{4}\frac{\widetilde{\rho}\widetilde{Y}_Z}{\widetilde{W}_Z}\widetilde{c}\frac{\widetilde{A}}{\widetilde{V}} \tag{3}$$

where $\widetilde{\gamma}_s$ is the radical quenching coefficient (or sticking coefficient, which is usually less than 0.1, depending on the surface properties as well as the fuel/air mixture) and $\widetilde{c}$ is the averaged random velocity of radical. For a tube, the surface-to-volume ratio is $\widetilde{A}/\widetilde{V}=4/\widetilde{d}$ with $\widetilde{d}$ being the tube diameter. In this study, the surface reaction is assumed to be thermally neutral and thereby the combustion heat release is reduced by radical loss on the wall (note that the completion reaction in Eq. (2) releases all the heat). It is noted that practically the radicals on the surface might recombine and re-enter the gas phase. The recombination and re-entering process is not considered in the present model. This is a limitation of the present model. Furthermore, as discussed in the Supplementary material, it might happen that there is not enough wall area to be able to sink enough radicals before saturation to have a significant effect on quenching. In the present model the saturation is assumed not to be reached. This is another limitation of the present model. Nevertheless, Saiki and Suzuki [46] showed that the channel-flame quenching process is limited by radical adsorption. Their simulation results indicated that there is enough wall area to be able to sink enough radicals before saturation even for their burned-stabilized channel-flame [46].

2.2. The model

We consider a quasi-one-dimensional (reduced from the integration of the two-dimensional model, following Zamashchikov and Minaev [8]), fuel lean, premixed flame propagating inside a tube (Fig. 1). For the sake of simplicity, we employ the diffusive–thermal model [41], in which the density as well as the thermal and transport properties of the mixture is assumed to be constant. Furthermore, uniform wall temperature is assumed and thereby heat recirculation [7,12,15] is not considered in the present model. Nevertheless, the heat exchange between gaseous mixture and tube wall is included. The heat flux is assumed to be proportional to the difference between local gas temperature $\widetilde{T}$ and wall temperature $\widetilde{T}_W$ (represented by the last term in Eq. (6). The effects of radiative loss, curvature, and stretch [42–44] are not included in the present model, which will be a subject for future study.

It should be emphasized that the quasi-one-dimensional model does not consider the radial temperature or concentration gradient. Due to the heat loss on the wall, the radical concentration near

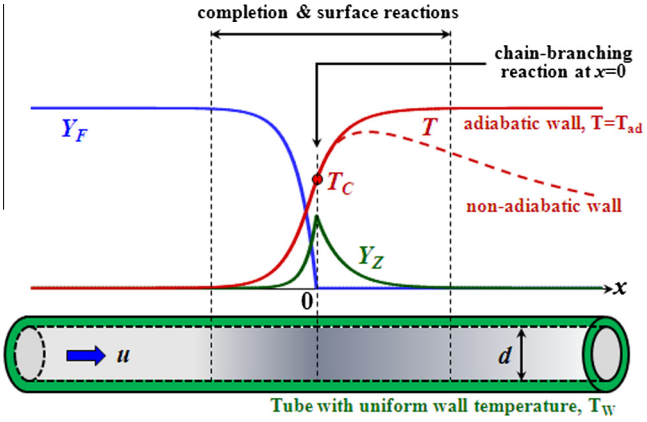

Fig. 1. The schematic flame structure.

the wall is in fact much lower than that at the center [26,46]. Consequently, our quasi-one-dimensional model might over-predict the influence of the wall-quenching of radicals. This is also a limitation of our model. In the coordinate attached to the propagating flame front, a steady model can be used to describe the propagating flame. The governing equations for mass fractions of fuel and radical as well as temperature are:

$$\widetilde{\rho}\widetilde{u}\frac{d\widetilde{Y}_F}{d\widetilde{x}}=\frac{d}{d\widetilde{x}}\left(\widetilde{\rho}\widetilde{D}_F\frac{d\widetilde{Y}_F}{d\widetilde{x}}\right)-\widetilde{W}_F\widetilde{\omega}_B \tag{4}$$

$$\widetilde{\rho}\widetilde{u}\frac{d\widetilde{Y}_Z}{d\widetilde{x}}=\frac{d}{d\widetilde{x}}\left(\widetilde{\rho}\widetilde{D}_Z\frac{d\widetilde{Y}_Z}{d\widetilde{x}}\right)+\widetilde{W}_Z(\widetilde{\omega}_B-\widetilde{\omega}_C-\widetilde{\omega}_W) \tag{5}$$

$$\widetilde{\rho}\widetilde{u}\widetilde{C}_P\frac{d\widetilde{T}}{d\widetilde{x}}=\frac{d}{d\widetilde{x}}\left(\widetilde{\lambda}\frac{d\widetilde{T}}{d\widetilde{x}}\right)+\widetilde{Q}\widetilde{\omega}_C-\frac{4\widetilde{\Omega}}{\widetilde{d}}(\widetilde{T}-\widetilde{T}_W) \tag{6}$$

where $\widetilde{u}$ is the inlet flow speed of the unburned mixture which is equal to the laminar flame propagation speed in the diffusive–thermal model. $\widetilde{D}_F$ and $\widetilde{D}_Z$ are the mass diffusion coefficients of the fuel and radical respectively, $\widetilde{C}_P$ the specific heat capacity of the mixture, $\widetilde{\lambda}$ the heat conductivity of the mixture, $\widetilde{Q}$ the specific heat release of the completion reaction, $\widetilde{\omega}$ the heat exchange coefficient, $\widetilde{d}$ the tube diameter, and $\widetilde{T}_W$ the wall temperature. The rates for the branching, completion, and surface-quenching reactions are given in Eqs. (1)–(3), respectively.Following Sharpe [33], we introduce the non-dimensional variables:

$$x=\frac{\widetilde{x}}{\widetilde{\delta}},\quad u=\frac{\widetilde{u}}{\widetilde{S}_u^0},\quad Y_F=\frac{\widetilde{Y}_F}{\widetilde{Y}_{F0}},\quad Y_Z=\frac{\widetilde{Y}_Z\widetilde{W}_F}{\widetilde{Y}_{F0}\widetilde{W}_Z},\quad T=\frac{\widetilde{T}}{\widetilde{T}_0},\quad T_W=\frac{\widetilde{T}_W}{\widetilde{T}_0} \tag{7}$$

where $\widetilde{Y}_{F0}$ is the fuel mass fraction in the unburned mixture and $\widetilde{T}_0=298K$ is the room temperature. The characteristic speed $\widetilde{S}_u^0$ and characteristic length $\widetilde{\delta}=\widetilde{\lambda}/(\widetilde{\rho}\widetilde{C}_P\widetilde{S}_u^0)$ are, respectively, the laminar flame speed and flame thickness of an adiabatic planar flame with initial temperature of $\widetilde{T}_0=298K$. The non-dimensional governing equations are:

$$u\frac{dY_F}{dx}=\frac{1}{Le_F}\frac{d^2Y_F}{dx^2}-\omega \tag{8}$$

$$u\frac{dY_Z}{dx}=\frac{1}{Le_Z}\frac{d^2Y_Z}{dx^2}+\omega-\Lambda Y_Z-\Gamma Y_Z \tag{9}$$

$$u\frac{dT}{dx}=\frac{d^2T}{dx^2}+Q\Lambda Y_Z-\Omega(T-T_W) \tag{10}$$

where $Le_F=\widetilde{\lambda}/(\widetilde{\rho}\widetilde{C}_P\widetilde{D}_F)$ and $Le_Z=\widetilde{\lambda}/(\widetilde{\rho}\widetilde{C}_P\widetilde{D}_Z)$ are the fuel and radical Lewis numbers, respectively. The non-dimensional heat release is given by $Q=\widetilde{Q}\widetilde{Y}_{F0}/(\widetilde{W}_F\widetilde{C}_P\widetilde{T}_0)$ and the non-dimensional adiabatic flame temperature is $T_{ad}=1+Q$. The non-dimensional heat exchange and radical quenching coefficients are respectively given by

$$\Omega=\frac{4\widetilde{\Omega}\widetilde{\delta}}{\widetilde{\rho}\widetilde{C}_P\widetilde{S}_u^0\widetilde{d}},\quad \Gamma=\frac{\widetilde{\gamma}_s\widetilde{c}\widetilde{\delta}}{\widetilde{S}_u^0\widetilde{d}} \tag{11}$$

Eq. (11) shows that both Ω and Γ increase with the decrease of tube diameter, $\widetilde{d}$, indicating that heat exchange and radical quenching becomes crucial for small scale combustion [1–4]. The radical quenching coefficient, Γ, depends on the temperature since the random velocity of radical, $\widetilde{c}$, is proportional to the square root of temperature. To simplify the problem, we assume that Γ is a constant to be specified ($\Gamma=0$ corresponds to an inert wall without surface quenching of radicals). For an adiabatic tube without wall quenching of radicals (i.e. $\Gamma=\Omega=0$), the governing Eqs. (8)–(10) reduce to those for an adiabatic planar flame [29,31,33] and we have $u=\widetilde{u}/\widetilde{S}_u^0=1$ when the initial temperature is $\widetilde{T}_0=298$ K.

In Eqs. (8) and (9), the non-dimensional branching reaction rate is [31]

$$\omega=\Lambda\Theta^2Y_FY_Z\exp\left[T_B\left(\frac{1}{T_C}-\frac{1}{T}\right)\right] \tag{12}$$

where $\Lambda=\widetilde{\lambda}\widetilde{A}_C/[\widetilde{C}_P(\widetilde{S}_u^0)^2\widetilde{W}]$ is the non-dimensional rate constant, $T_B=\widetilde{T}_B/\widetilde{T}_0$ the non-dimensional activation temperature, $T_C=\widetilde{T}_C/\widetilde{T}_0$ the non-dimensional in-homogenous chain-branching crossover temperature [31], and $\Theta=T_B/T_C$. In the asymptotic limit of high activation energy ($T_B\to\infty$), the chain-branching reaction is confined in an infinitesimally thin reaction sheet at $x=x_f=0$. As shown in Fig. 1, no chain-branching reaction occurs on either side of this reaction sheet (i.e. $\omega=0$ when $x\neq0$). According to the asymptotic analysis by Dold [31], the following conditions must hold across or at $x=x_f=0$:

$$[Y_F]=[Y_Z]=[T]=\left[\frac{dT}{dx}\right]=\left[\frac{1}{Le_F}\frac{dY_F}{dx}+\frac{1}{Le_Z}\frac{dY_Z}{dx}\right]=T-T_C=Y_F=0 \tag{13}$$

where the square brackets denote the difference between the variables on the unburned and burned sides, i.e. $[f]=f(x=0^-)-f(x=0^+)$.

The boundary conditions are specified as

$$x\to-\infty:\quad T=T_W,Y_F=1,Y_Z=0 \tag{14}$$

$$x\to+\infty:\quad dT/dx=0,Y_F=0,dY_Z/dx=0 \tag{15}$$

It is noted that according to Eq. (14), the temperature of unburned gas is set to be the same as the wall temperature even for an adiabatic tube (i.e. $\Omega=0$). Therefore, the temperature of gaseous mixture is always equal to or higher than that of the wall, and there is heat loss to the wall when $\Omega>0$. When $T_W=\widetilde{T}_W/\widetilde{T}_0>1$, the unburned mixture is heated to $T=T_W$.

In order to simultaneously satisfy the conditions at $x=x_f=0$ in Eq. (13) and boundary conditions at $x\to\pm\infty$ in Eqs. (14) and (15), the variable, Λ, must have a specific value [33]. Therefore, Λ is an eigenvalue related to the flame speed [33]. It is determined by the condition that $u=\widetilde{u}/\widetilde{S}_u^0=1$ when $T_W=1$ (i.e., $\widetilde{T}_W=\widetilde{T}_0=298K$, the unburned mixture is at room temperature) and $\Omega=\Gamma=0$ (without heat and radical loss). The eigenvalue Λ is given implicitly by [33]:

$$\Lambda Le_Z=\left(1+\frac{1-T_C}{Q}\right)(S_2^2-S_2)(S_1-S_2),$$
$$S_{1,2}=\frac{Le_Z\pm\sqrt{Le_Z^2+4\Lambda Le_Z}}{2} \tag{16}$$

which can be solved using iteration method.

2.3. Analytical solution

Under the reaction sheet assumption ($\omega = 0$ for $x < 0$ and $x > 0$), Eqs. (8)–(10) together with conditions in Eqs. (13)–(15) can be solved analytically in the unburned and burned zones. The fuel mass fraction in the burned zone is zero according to the fuel lean assumption. Therefore, the distribution for fuel mass fraction is obtained as

$$Y_F(x) = \begin{cases} 1 - \exp(uLe_F x) & if \quad x \le 0 \\ 0 & if \quad x \ge 0 \end{cases} \tag{17}$$

The solution for radical mass fraction is

$$Y_Z(x) = \begin{cases} Y_{Zf}\exp(\lambda_1 x) & if \quad x \le 0 \\ Y_{Zf}\exp(\lambda_2 x) & if \quad x \ge 0 \end{cases} \tag{18}$$

where $\lambda_{1,2} = [uLe_Z \pm \sqrt{(uLe_Z)^2 + 4Le_Z(\Lambda + \Gamma)}]/2$ and Y_{Zf} is the radical mass fraction at the flame front ($x = 0$). Substituting Eqs. (17) and (18) into the requirement of $[Le_F^{-1}dY_F/dx + Le_Z^{-1}dY_Z/dx] = 0$ at $x = 0$ in Eq. (13) yields

$$Y_{Zf} = \frac{uLe_Z}{\lambda_1 - \lambda_2} = \frac{uLe_Z}{\sqrt{(uLe_Z)^2 + 4Le_Z(\Lambda + \Gamma)}} \tag{19}$$

The temperature distribution is obtained as

$$T(x) = \begin{cases} T_W + (T_C - T_W)e^{\gamma_1 x} - \frac{Q\Lambda Y_{Zf}[e^{\lambda_1 x} - e^{\gamma_1 x}]}{\lambda_1^2 - u\lambda_1 - \Omega} & if \quad x \le 0 \\ T_W + (T_C - T_W)e^{\gamma_2 x} - \frac{Q\Lambda Y_{Zf}[e^{\lambda_2 x} - e^{\gamma_2 x}]}{\lambda_2^2 - u\lambda_2 - \Omega} & if \quad x \ge 0 \end{cases} \tag{20}$$

where $\gamma_{1,2} = [u \pm \sqrt{u^2 + 4\Omega}]/2$.

Substituting Eq. (20) into the requirement of heat flux continuity ($[dT/dx] = 0$ at $x = 0$ in Eq. (13) yields the following correlation describing the flame propagation in a tube with heat loss to and radical quenching on the wall:

$$(\gamma_1 - \gamma_2)\frac{T_C - T_W}{Q} = \Lambda Y_{Zf}\left(\frac{1}{\lambda_1 - \gamma_2} + \frac{1}{\gamma_1 - \lambda_2}\right) \tag{21}$$

By numerically solving the above correlation using Newton's iterative method, we can get the flame propagation speed, u, as a function of Ω, Γ, Le_Z, T_C, T_W, and Q. As mentioned before, the coefficient Λ is obtained from Eq. (16). By substituting the solution into Eqs. (17)–(20), the distributions for fuel mass fraction, radical mass fraction, and temperature can be readily obtained. Therefore, the present theory can be used to investigate flame propagation in a tube with thermal and/or radical quenching ($\Omega > 0$ and/or $\Gamma > 0$) at different radical Lewis numbers (Le_Z), cross-over temperatures (T_C), wall temperatures (T_W), and tube diameters (the influence of tube diameter is represented by Ω and Γ, as indicated by Eq. (11).

In the limit of $T_W = 1$ and $\Gamma = \Omega = 0$, Eq. (21) describes the propagation of an adiabatic planar flame and it reduces to Eq. (16) which is used to determine the eigenvalue Λ.

In the limit of $T_W = 1$ and $\Gamma = 0$ (i.e. without radical quenching), Eq. (21) reduces to the correlation derived by Dold and coworkers [29,31] for a premixed planar flame with linear heat loss. By solving Eq. (21) with $T_W = 1$ and $\Gamma = 0$, the flammability limit or quenching diameter due to heat loss can be determined.

In the limit of $T_W = 1$ and $\Omega = 0$ (i.e. without heat loss), Eq. (21) reduces to

$$u\frac{T_C - 1}{Q} = \Lambda Y_{Zf}\left(\frac{1}{\lambda_1} + \frac{1}{u - \lambda_2}\right) \tag{22}$$

which can be used to determine the flammability limit or quenching diameter due to radical loss.

3. Results and discussion

The fuel Lewis number, Le_F, is not included in Eq. (21) since the normalized flame propagation speed of an unstretched planar flame is independent of Le_F [31,33]. (For stretched flames, the fuel and radical Lewis numbers both affect the flame propagation speed [38–40].) The fuel Lewis number only affects the distribution of fuel mass fraction, as indicated by Eq. (17). It is noted the fuel Lewis strongly affects the instability of flame propagation: diffusional–thermal cellular instability occurs for a fuel Lewis number lower than unity; while diffusional–thermal pulsating instability happens at large fuel Lewis number and large Zel'dovich number [47]. In this study, a one-dimensional flame is considered and therefore the diffusional–thermal cellular instability is not included. Moreover, in the present study we fix the fuel Lewis number to be unity ($Le_F = 1$) and thus the pulsating instability does not occur. As part of future work, stability analysis [31,33] needs to be conducted to understand the instability of the flame propagation in a tube. According to Eqs. 21, 16, and 22, the flame propagation speed is affected by $(T_C - 1)/Q$ and $(T_W - 1)/Q$. Therefore, the same results for different values of Q can be obtained through adjusting the values of T_C and T_W. Here we present results for different values of T_C and/or T_W with the non-dimensional heat release fixed to be $Q = 5$ (i.e. the adiabatic flame temperature is about 1800 K).

Figure 2 plots the distributions of normalized temperature, defined as $\theta = (T - 1)/Q$, as well as fuel and radical mass fractions for three different cases with the same flame propagation speed of $u = 0.7$. The results (denoted by solid lines) for an adiabatic flame without radical quenching (for which $\Omega = \Gamma = 0$ and $u = 1.0$) are shown together for comparison. Figure 2 indicates that the flame structure is similar for these three cases and that the flame propagation speed can be reduced by heat loss only ($\Omega > 0$, $\Gamma = 0$), radical

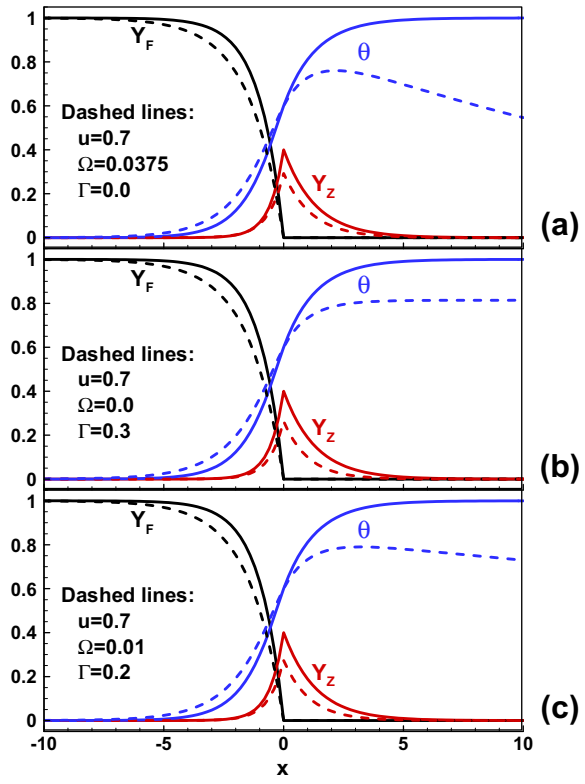

Fig. 2. The flame structure for $Le_Z = 1$, $T_C = 4.0$, and $T_W = 1.0$. The solid lines denote results without heat loss or radical quenching ($\Gamma = \Omega = 0$ and thus $u = 1.0$). The dashed lines denote results at fixed flame speed of $u = 0.7$ with (a) heat loss only, (b) radical quenching only, and (c) both heat loss and radical quenching.

quenching only ($\Gamma > 0$, $\Omega = 0$), or a combination of heat loss and radical quenching ($\Omega > 0$, $\Gamma > 0$). Therefore, the present theoretical model can be used to study both the thermal and kinetic quenching mechanisms. When there is heat loss or/and radical quenching, Fig. 2 shows that both the radical concentration and temperature are reduced.

Using the theory presented in Section 2, we investigate the flame propagation and extinction in a tube with heat loss and/or radical quenching on the wall. The effects of radical Lewis number, cross-over temperature, wall temperature, and tube diameter are discussed in the following.

3.1. Effects of radical Lewis number

In this subsection, the cross-over temperature is fixed to be $T_C = 4.0$ and the wall is at room temperature ($T_W = 1.0$). Figure 3 presents the flame structure at different radical Lewis numbers for an adiabatic flame without radical quenching ($\Omega = \Gamma = 0$). With the decrease of radical Lewis number, the mass diffusivity of radical increases and thereby the distribution of radical mass fraction becomes broader. Similar change in the temperature distribution is observed since the combustion heat release is proportional to the radical concentration (see the second term on the right hand side of Eq. (10).

Figure 3 shows that the same temperature, $T = T_C = 4.0$ (i.e. $\theta = (T_C - 1)/Q = 0.6$) occurs at the reaction sheet, $x = x_f = 0$, where the chain-branching reaction takes place. If the temperature cannot reach the cross-over temperature due to heat and/or radical losses, the chain-branching reaction does not take place and the flame is quenched. Therefore, the heat and/or radical losses on the upstream of the reaction sheet (i.e. $x \leqslant 0$) directly influence the flame speed and extinction limit. Integrating the radical mass fraction given in Eqs. (18) and (19) yields the following expression for the total amount of radical in the region of $x \leqslant 0$:

$$\int_{-\infty}^{0} Y_Z(x)dx = \frac{Y_{Zf}}{\lambda_1} = \frac{2}{\sqrt{(uLe_Z)^2 + 4Le_Z(\Lambda+\Gamma)} + uLe_Z + 4(\Lambda+\Gamma)/u} \quad (23)$$

Eq. (23) indicates that $\int_{-\infty}^{0} Y_Z(x)dx$ monotonically decreases with Le_Z. Therefore, with the decrease of Le_Z, more radical appears at the upstream of the reaction sheet. Consequently, the influence of radical quenching is expected to be stronger at smaller Le_Z. Furthermore, with the decrease of Le_Z, the temperature rise becomes larger at $x \leqslant 0$ (as demonstrated in Fig. 3) and there is more heat loss. Therefore, the influence of heat loss is also expected to be stronger at smaller Le_Z.

According to above discussions, the influence of thermal quenching mechanism and that of kinetic quenching mechanism both become stronger with the decrease of radical Lewis number. This is demonstrated by Fig. 4 which shows the change of flame speed with the heat loss and radical quenching coefficients. In Fig. 4(a), there are two branches in the u–Ω diagram. Physical flame propagation can occur only for the upper branch; the lower branch represents unstable solutions. Similar results were obtained by Dold [31] considering two-step chemistry and in theory considering one-step global chemistry [47]. The turning point (denoted by open circle) corresponds to the maximum value of heat loss coefficient (referred to as the critical heat loss coefficient, Ω_C), at which extinction limit is reached. Similar results for non-adiabatic flame without wall quenching of radicals (i.e. $\Omega > 0$, $\Gamma = 0$) were reported by Dold et al. [29,31]. With the increase of radical quenching coefficient, both the flame propagation speed and the critical heat loss coefficient, Ω_C, become smaller since flame is weakened by radical quenching. With the decrease of the Le_Z, the flame is shown to have smaller flame speed and be more easily to be quenched. This is due to the reason mentioned in the previous paragraph.

Similarly, Fig. 4(b) shows that for a given value of $\Omega > 0$, there is a critical radical quenching coefficient, Γ_C, beyond which flame

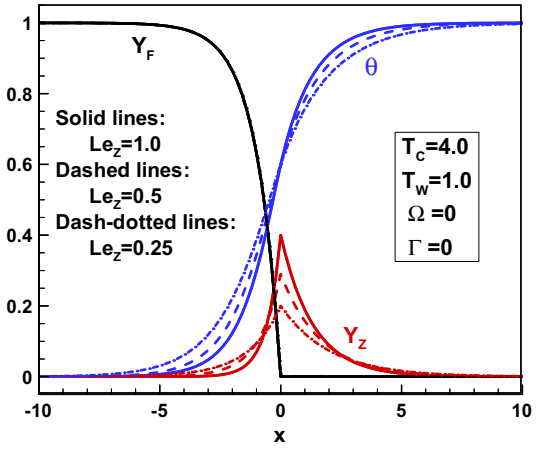

Fig. 3. The flame structure at different radical Lewis numbers.

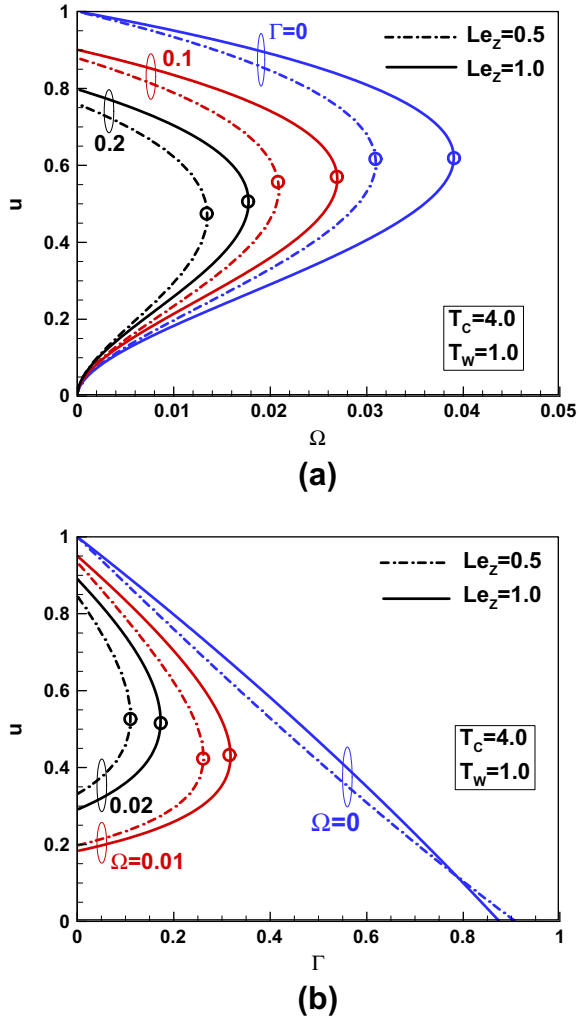

Fig. 4. Change of the flame speed with the (a) heat loss coefficient and (b) radical quenching coefficient at different radical Lewis numbers.

extinction occurs with finite flame speed. As expected, with the decrease of Le_Z, the flame is shown to be more easily quenched and have a smaller Γ_C. When there is no heat loss ($\Omega = 0$) and only exists radical loss, Fig. 4(b) shows that there is no turning point and the flame speed decreases monotonically with the radical quenching coefficient. At $\Omega = 0$ and $\Gamma = \Gamma_C$, flame extinction occurs with zero flame speed and the maximum temperature is equal to the cross-over temperature. This is different from the flammability limit caused by heat loss, at which flame extinction occurs with finite flame speed and the maximum temperature is above the cross-over temperature. Similar observation was discussed in recent study by Kurdyumov and Fernandez-Galisteo [45]. It should be emphasized that the radical quenching effect and thermal quenching effect exist simultaneously in practical experiments. Theoretically, for an adiabatic case without thermal quenching effect, the flame could be quenched solely by radical quenching effect. In experiments, however, this is difficult to realize since heat loss always exists. With the decrease of the tube diameter, the flame will be first extinguished due to thermal quenching. Figure 5 shows the heat loss and radical quenching limits at different radical Lewis numbers. Flame propagation happens only when the heat loss and radical quenching coefficients are below the lines shown in Fig. 5. Both the thermal quenching limit, Ω_C, and the kinetic quenching limit, Γ_C, decrease with the decrease of Le_Z, and the flame extinction region becomes broader at smaller Le_Z. Moreover, compared to the radical quenching limit, the heat loss quenching limit is shown to be more strongly affected by Le_Z. This is due to the fact that heat loss directly reduces the temperature and thereby it can terminate the chain-branching reaction by making the temperature below the cross-over temperature.

3.2. Effects of cross-over temperature

Here the radical Lewis number and wall temperature are both fixed to be unity ($Le_Z = T_W = 1.0$). Figure 6 shows the distributions of normalized temperature, $\theta = (T - 1)/Q$, fuel mass fraction, Y_F, and radical mass fraction, Y_Z, at three different cross-over temperatures for an adiabatic flame without radical quenching ($\Omega = \Gamma = 0$). The cross-over temperature does not affect the distribution of fuel mass fraction. However, as shown in Fig. 6, the cross-over temperature has great influence on the radical mass fraction and temperature. At higher cross-over temperature, less radical can be produced and the temperature increases more sharply. Therefore, it is expected that the influence of radical quenching is weaker at higher cross-over temperature.

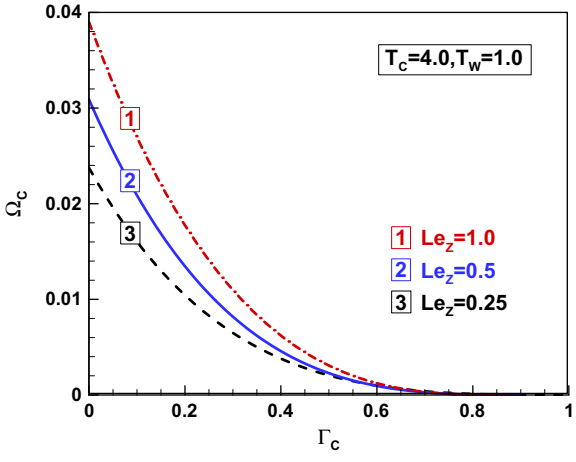

Fig. 5. Effects of radical Lewis number on flame quenching limits. Flame quenching occurs when the coefficients of (Γ, Ω) are on the upper-right side of each line.

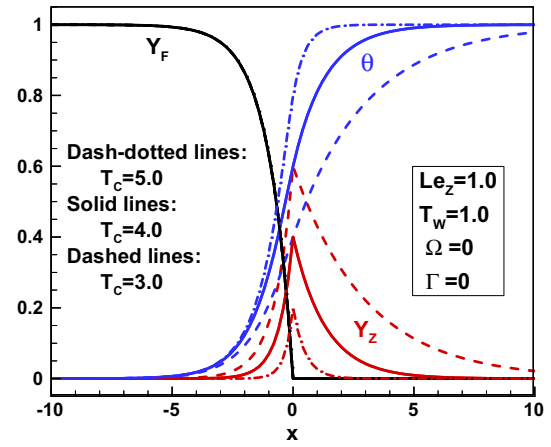

Fig. 6. The flame structure at different cross-over temperatures.

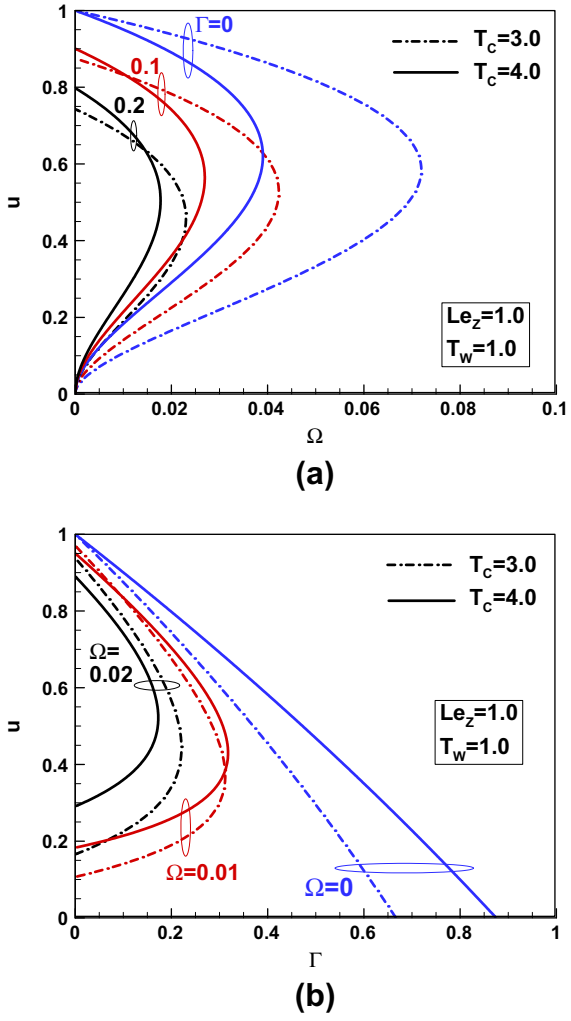

Fig. 7. Change of the flame speed with the (a) heat loss coefficient and (b) radical quenching coefficient at different cross-over temperatures.

Figure 7 shows the change of the flame speed with the heat loss and radical quenching coefficients. When there is no radical quenching ($\Gamma = 0$), Fig. 7(a) shows that the flame can be more easily quenched and have a smaller value of Ω_C at higher cross-over temperature, T_C. This is reasonable since the chain-branching

reaction takes place only when the temperature is above the cross-over temperature, and the maximum temperature can be more easily reduced to be below the cross-over temperature by heat loss at higher T_C. When there is no heat loss ($\Omega = 0$), Fig. 7(b) shows that the flame becomes more difficult to be quenched and has a larger value of Γ_C at higher cross-over temperature. This is because less amount of radical exists at higher T_C, as shown in Fig. 6. Therefore, increasing the cross-over temperature has two opposite effects: it promotes extinction caused by thermal quenching mechanism, while it inhibits extinction caused by kinetic quenching mechanism. At $\Gamma = 0.1$ and small value of Ω (say $\Omega = 0.005$), the kinetic quenching mechanism dominates over the thermal mechanism, and thereby Fig. 7(a) shows that the flame speed at $T_C = 4.0$ is higher than that at $T_C = 3.0$. However, at $\Gamma = 0.1$ and large value of Ω (say $\Omega = 0.02$), the thermal mechanism dominates over the kinetic quenching mechanism, and thereby Fig. 7(a) and (b) show that the flame speed is lower and the flame is more easily quenched at higher cross-over temperature.

These two competing effects caused by changing the cross-over temperature are further demonstrated by results in Fig. 8, which shows the heat loss and radical quenching limits at three different cross-over temperatures. Flame extinction occurs when the coefficients of (Γ, Ω) are on the upper-right side of each line. Fig. 8 indicates that the thermal quenching limit, Ω_C, reduces with the increase of the cross-over temperature, while the kinetic quenching limit, Γ_C, increases with T_C. This observation is consistent with discussions mentioned above.

3.3. Effects of wall temperature

Figure 9 shows the flame structure at different wall temperatures for $Le_Z = 1.0$, $T_C = 4.0$ and $\Omega = \Gamma = 0$. As mentioned before, according to Eq. (14), the initial temperature of unburned gas is set to be the same as the wall temperature even for an adiabatic tube (i.e. $\Omega = 0$). Therefore, the results in Fig. 9 are in fact for different initial temperatures of unburned gas. Figure 9 indicates that with the increase of the initial unburned gas temperature, the radical profile has not only a higher peak, but also a wider distribution. Therefore, it is expected that the influence of radical quenching on the wall becomes stronger at higher initial unburned gas temperature (or higher wall temperature).

Figure 10 demonstrates the effects of heat loss and radical quenching on flame speed and extinction at different wall temperatures. With the increase of the wall temperature, the initial temperature of unburned gas also increases and hence the flame propagation is greatly enhanced. The flame speed is shown to become much larger at higher wall temperature. Consequently, both the heat loss quenching limit, Ω_C, and the radical quenching limit, Γ_C, are significantly extended by the increase of wall temperature, as demonstrated by Fig. 11. Similar observation was found in

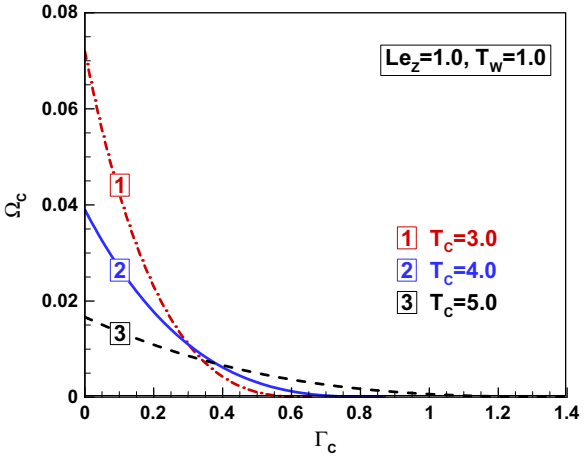

Fig. 8. Effects of cross-over temperature on flame quenching limits. Flame quenching occurs when the coefficients of (Γ, Ω) are on the upper-right side of each line.

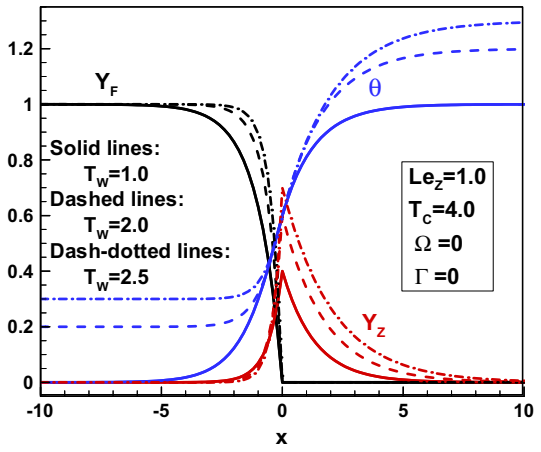

Fig. 9. The flame structure at different wall temperatures.

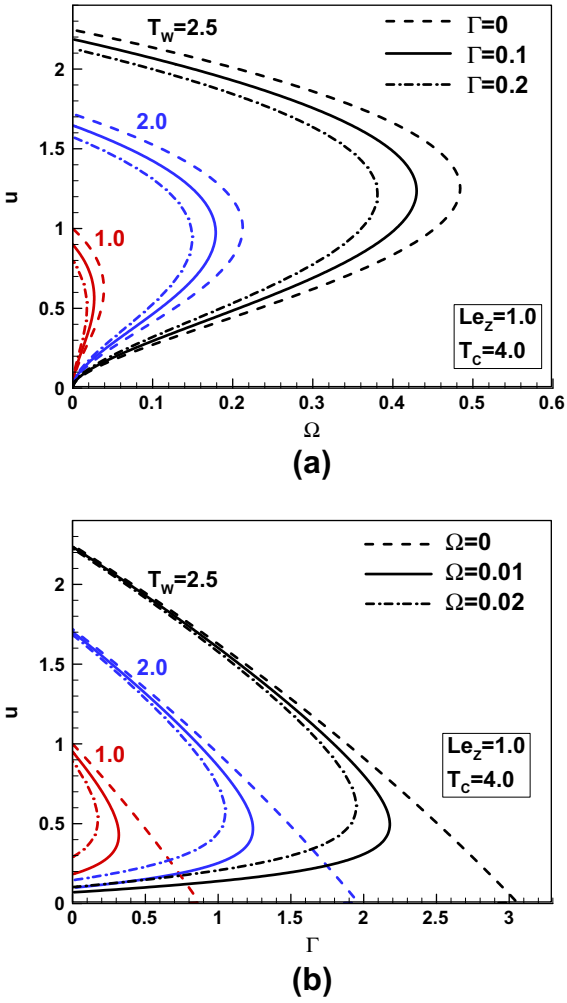

Fig. 10. Change of the flame speed with the (a) heat loss coefficient and (b) radical quenching coefficient at different wall temperatures.

simulations considering radical quenching on the wall [26]. According the results in Figs. 10 and 11, when there is no radical quenching ($\Gamma = 0$), the ratio between heat loss quenching limits at $T_W = 2.0$ and $T_W = 1.0$ is $\Omega_C(T_W = 2.0)/\Omega_C(T_W = 1.0) = 5.45$. Similarly, when there is no heat loss ($\Omega = 0$), the ratio between radical quenching limits at $T_W = 2.0$ and $T_W = 1.0$ is $\Gamma_C(T_W = 2.0)/\Gamma_C(T_W = 1.0) = 2.25$. Therefore, compared to the radical quenching limit, the heat loss quenching limit is much more extended by the increase of wall temperature. The quenching limit caused by heat loss is due to the fact that the chain-branching reaction does not take place when the temperature is below the cross-over temperature. Therefore, increasing the wall temperature (or initial temperature of unburned gas) is very effective in extending the heat loss quenching limit. This is in fact used in small scale combustion for which the flammability limit and quenching diameter are greatly extended through heat recirculation [7,12,15].

3.4. Effects of tube diameter

In the results discussed above, the heat loss coefficient, Ω, and radical quenching coefficient, Γ, change independently. According to Eq. (11), with the decrease of the tube diameter, both Ω and Γ increase while the ratio between them remains unchanged. Therefore, in this subsection, we investigate the effects of tube diameter by changing the heat loss coefficient, Ω, while keeping the ratio, Γ/Ω, unchanged. According to Eq. (11), the ratio, Γ/Ω, is proportional to the radical quenching coefficient (or sticking coefficient) $\tilde{\gamma}_s$. Our rough estimation shows that Γ/Ω is around 500–1000 times of $\tilde{\gamma}_s$ for typical fuel/air mixtures. In the following we use three values, $\Gamma/\Omega = 0$, 5, and 20, to cover a wide range of Γ/Ω (which is determined by the value of $\tilde{\gamma}_s$). Since the theory works for all different values of Γ/Ω, the same conclusion can be drawn even when other values of Γ/Ω (say, $\Gamma/\Omega = 0.1$) are used.

Figure 12(a) plots the flame speed as a function of heat loss coefficient for fixed values of Γ/Ω. When $\Gamma/\Omega = 0$, there is no radical quenching on the wall and only heat loss is considered. Since the heat loss coefficient, Ω, is inversely proportional to the square of the tube diameter, the turning points in Fig. 12(a) correspond to the quenching diameter, below which flame extinction happens. As expected, Fig. 12(a) shows that the quenching diameter increases with the wall temperature. By comparing results without radical quenching ($\Gamma/\Omega = 0$) with those including radical quenching ($\Gamma/\Omega = 5$) in Fig. 12(a), we find that the radical quenching reduces flame speed and helps to extinguish the flame. As a result,

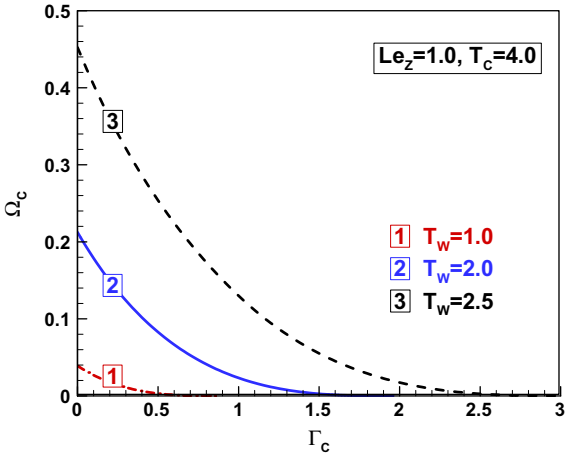

Fig. 11. Effects of wall temperature on flame quenching limits. Flame quenching occurs when the coefficients of (Γ, Ω) are on the upper-right side of each line.

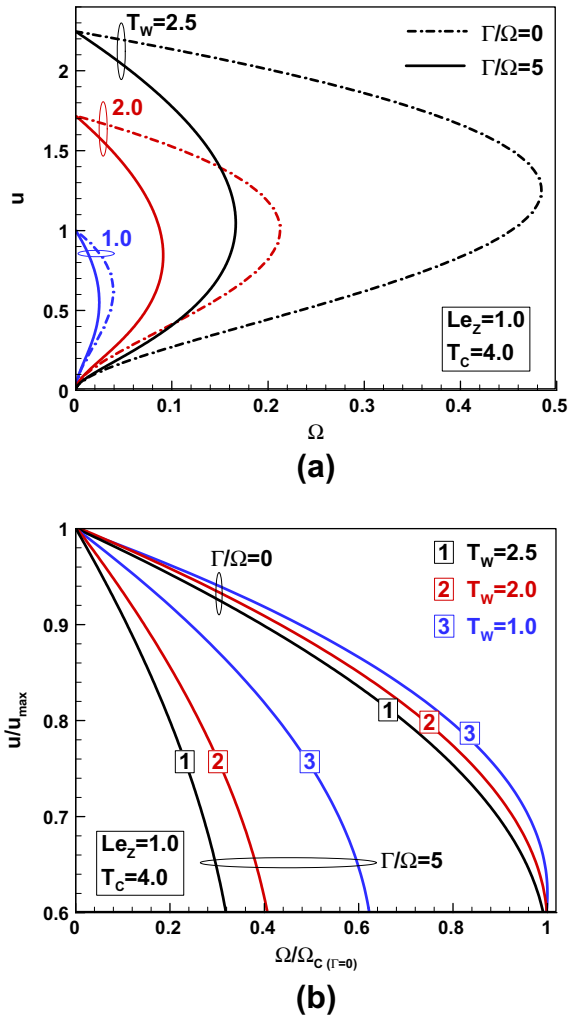

Fig. 12. Change of the flame speed with heat loss coefficient at fixed value of Γ/Ω.

Fig. 12(a) indicates that the quenching diameter is significantly reduced by the radical quenching effect.

To demonstrate the effects of wall temperature, we normalize the flame speed u by u_{max} (the speed at $\Omega = 0$) and the heat loss coefficient Ω by Ω_C (the heat loss quenching limit). The results are shown in Fig. 12(b). It is observed that the difference between results without radical quenching ($\Gamma/\Omega = 0$) and those with radical quenching ($\Gamma/\Omega = 5$) is larger at higher wall temperature. Therefore, radical quenching plays a more crucial role at higher wall temperature. The same conclusion was drawn from numerical simulation [26] and experiments [27,46]. This is mainly due to the fact that the radical concentration becomes larger at higher initial unburned gas temperature (which is equal to the wall temperature), as shown in Fig. 9.

Figure 13 shows the change of heat loss quenching limit with wall temperature for different values of Γ/Ω. Transient numerical simulation considering finite rate of the chain-branching reaction indicates that the stable flame propagation cannot be observed when the wall temperature is close to the chain-branching cross-over temperature. Therefore, in Fig. 13 the maximum wall temperature is $T_W = 3$, which is lower than the cross-over temperature $T_C = 4$. With the increase of the wall temperature, the initial temperature of unburned gas also increases. Therefore, the quenching limit shown in Fig. 13(a) is significantly extended by the increase of wall temperature, indicating that the quenching diameter decreases with the wall temperature. In Fig. 13(b), the normalized

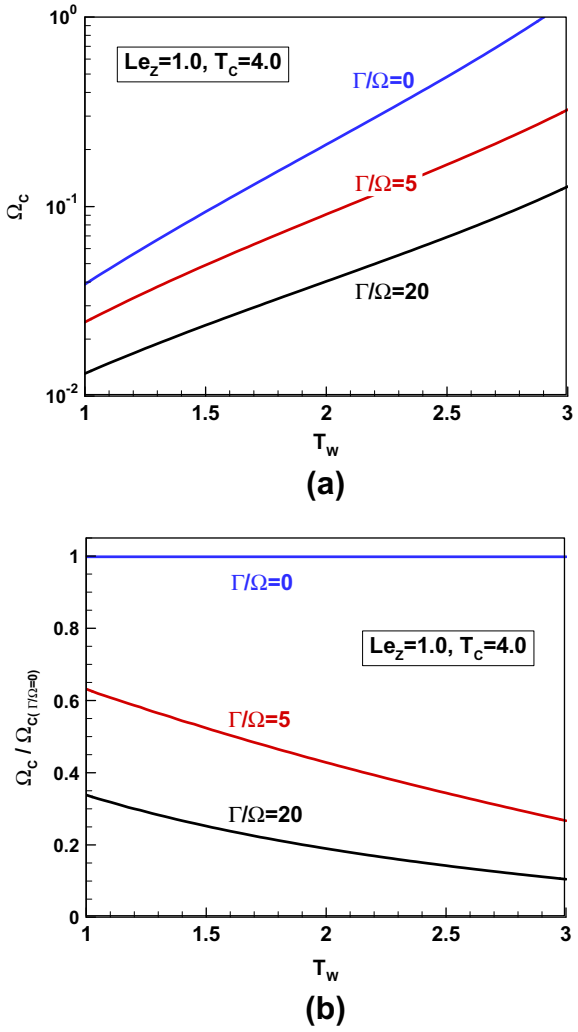

Fig. 13. Change of the flame quenching limit with wall temperature at fixed value of Γ/Ω.

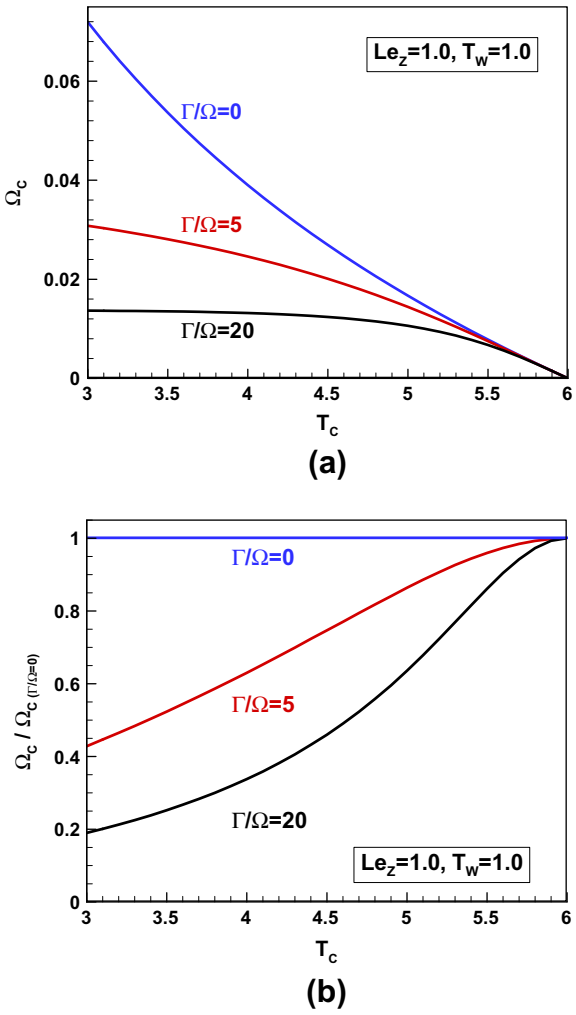

Fig. 14. Change of the flame quenching limit with cross-over temperature at fixed value of Γ/Ω.

heat loss quenching limit, $\Omega_C/\Omega_{C(\Gamma/\Omega=0)}$ is presented. The difference between Ω_C without radical quenching ($\Gamma/\Omega = 0$) and that with radical quenching ($\Gamma/\Omega = 5$ or 20) is caused by radical quenching and it is shown to increase with the wall temperature. Therefore, this further demonstrates that radical quenching plays a more crucial role at higher wall temperature. This is mainly due to the fact that the radical concentration becomes larger at higher initial unburned gas temperature (which is equal to the wall temperature), as shown in Fig. 9.

Similarly, Fig. 14 shows the change of heat loss quenching limit with cross-over temperature for different values of Γ/Ω. As discussed in Section 3.2, the flame is more easily quenched by heat loss at higher cross-over temperature. Therefore, in Fig. 14(a) the heat loss quenching limit is shown to monotonically decreases with the cross-over temperature, indicating that the quenching diameter increases with the cross-over temperature. When radical quenching effects are included, the heat loss quenching limit is reduced. The influence of radical quenching at different cross-over temperatures is demonstrated in Fig. 14(b). The normalized heat loss quenching limit, $\Omega_C/\Omega_{C(\Gamma/\Omega=0)}$, is shown to monotonically increase with the cross-over temperature, indicating that the influence of radical quenching becomes weaker at higher cross-over temperature. This is because the radical concentration becomes smaller at higher cross-over temperature, as shown in Fig. 6. Similar phenomena were observed in numerical simulation of channel flame with wall quenching of radicals [26].

Therefore, according to the above discussions, the flame speed decreases with the decrease of tube diameter (increase of heat loss coefficient Ω) and flame extinction occurs when the quenching diameter is reached. Furthermore, influence of radical quenching increases with the wall temperature while it decreases with the cross-over temperature.

4. Conclusions

To provide an incremental advance to former analytical models, in this study we develop a quasi-one-dimensional theoretical model describing flame propagation in a tube with heat loss and radical quenching on the wall. The thermally sensitive intermediate kinetics and surface radical quenching reaction are included in the present model. In the asymptotic limit of large activation energy for the chain-branching reaction, an analytical correlation is derived to describe the change of flame speed with heat loss and radical quenching coefficients. Based on this correlation, the effects of radical Lewis number, wall temperature, cross-over temperature, and tube diameter on flame speed and quenching limit are examined. The main conclusions are:

1. With the decrease of radical Lewis number, higher radical production and larger temperature rise occur at the upstream of the reaction sheet. Therefore, the influence of thermal quenching mechanism and that of kinetic quenching mechanism both become stronger with the decrease of radical Lewis number. When there is no heat loss and only radical quenching is considered, flame extinction occurs with zero flame speed. This is different from the flammability limit caused by heat loss, at which flame extinction occurs with finite flame speed.
2. With the increase of cross-over temperature, fewer radicals are produced and thereby the influence of radical quenching becomes weaker at higher cross-over temperature. Meanwhile, the flame can be more easily quenched by heat loss at higher cross-over temperature. Therefore, increasing the cross-over temperature has two opposite effects: it promotes extinction caused by thermal quenching mechanism, while it inhibits extinction caused by kinetic quenching mechanism.
3. The initial temperature of unburned gas is set to be the same as the wall temperature. With the increase of the wall temperature, both the heat loss quenching limit and the radical quenching limit are significantly extended. Furthermore, compared to the radical quenching limit, the heat loss quenching limit is much more extended by the increase of wall temperature. Therefore, in small scale combustion the flammability limit and quenching diameter can be greatly extended by heat recirculation.
4. With the decrease of the tube diameter, the heat loss and radical quenching coefficients both increase while the ratio between them remains unchanged. The quenching diameter can be greatly reduced by the increase of wall temperature or the decrease of cross-over temperature. Moreover, the influence of radical quenching is found to increase with the wall temperature and to decrease with the cross-over temperature. These conclusions drawn from theoretical analysis are consistent with numerical results [26] and experimental observations [27,46] reported in the literature.

Acknowledgments

This work was supported by National Natural Science Foundation of China (Nos. 51136005 and 50976003), Doctoral Fund of Ministry of Education of China (Nos. 20120001110080 and 20100001120003), and Key Laboratory of Low-grade Energy Utilization Technologies and Systems at Chongqing University (No. LLEUTS 201304). We thank the reviewers for providing constructive comments which help to improve the paper.

Appendix A. Supplementary material

Supplementary data associated with this article can be found, in the online version, at http://dx.doi.org/10.1016/j.combustflame.2013.07.008.

References

[1] A.C. Fernandez-Pello, Proc. Combust. Inst. 29 (2003) 883–899.
[2] Y.G. Ju, K. Maruta, Prog. Energy Combust. Sci. 37 (2011) 669–715.
[3] K. Maruta, Proc. Combust. Inst. 33 (2011) 125–150.
[4] N.S. Kaisare, D.G. Vlachos, Prog. Energy Combust. Sci. 38 (2012) 321–359.
[5] D.B. Spalding, Proc. R. Soc. Lon. Ser. A – Math. Phys. Sci. 240 (1957) 83–100.
[6] B. Lewis, G. Von Elbe, Combustion Flames and Explosive of Gases, Academic Press, New York, 1961.
[7] S.A. Lloyd, F.J. Weinberg, Nature 251 (1974) 47–49.
[8] V.V. Zamashchikov, S.S. Minaev, Combust. Explos. Shock Waves 37 (2001) 21–26.
[9] R.V. Fursenko, S.S. Minaev, V.S. Babkin, Combust. Explos. Shock Waves 37 (2001) 493–500.
[10] P.D. Ronney, Combust. Flame 135 (2003) 421–439.
[11] Y.G. Ju, C.W. Choi, Combust. Flame 133 (2003) 483–493.
[12] Y.G. Ju, B. Xu, Proc. Combust. Inst. 30 (2005) 2445–2453.
[13] K. Maruta, T. Kataoka, N.I. Kim, S. Minaev, R. Fursenko, Proc. Combust. Inst. 30 (2005) 2429–2436.
[14] N.I. Kim, S. Kato, T. Kataoka, T. Yokomori, S. Maruyama, T. Fujimori, K. Maruta, Combust. Flame 141 (2005) 229–240.
[15] I. Schoegl, J.L. Ellzey, Combust. Flame 151 (2007) 142–159.
[16] S. Minaev, K. Maruta, R. Fursenko, Combust. Theory Modell. 11 (2007) 187–203.
[17] C.H. Kuo, P.D. Ronney, Proc. Combust. Inst. 31 (2007) 3277–3284.
[18] A. Fan, S. Minaev, E. Sereshchenko, R. Fursenko, S. Kumar, W. Liu, K. Maruta, Proc. Combust. Inst. 32 (2009) 3059–3066.
[19] H. Nakamura, A.W. Fan, S. Minaev, E. Sereshchenko, R. Fursenko, Y. Tsuboi, K. Maruta, Combust. Flame 159 (2012) 1631–1643.
[20] C.H. Chen, P.D. Ronney, Proc. Combust. Inst. 33 (2011) 3285–3291.
[21] P. Popp, M. Smooke, M. Baum, Proc. Combust. Inst. 26 (1996) 2693–2700.
[22] P. Popp, M. Baum, Combust. Flame 108 (1997) 327–348.
[23] P. Aghalayam, D.G. Vlachos, AICHE J. 44 (1998) 2025–2034.
[24] P. Aghalayam, P.A. Bui, D.G. Vlachos, Combust. Theory Modell. 2 (1998) 515–530.
[25] S. Raimondeau, D. Norton, D.G. Vlachos, R.I. Masel, Proc. Combust. Inst. 29 (2003) 901–907.
[26] Y.G. Ju, B. Xu, AIAA-2006-1351.
[27] C.M. Miesse, R.I. Masel, C.D. Jensen, M.A. Shannon, M. Short, AICHE J. 50 (2004) 3206–3214.
[28] H.L. Yang, Y.X. Feng, Y.Y. Wu, X.H. Wang, L.Q. Jiang, D.Q. Zhao, H. Yamashita, Combust. Sci. Technol. 183 (2011) 444–458.
[29] J.W. Dold, R.W. Thatcher, A. Omon-Arancibia, J. Redman, Proc. Combust. Inst. 29 (2002) 1519–1526.
[30] J.W. Dold, R.O. Weber, R.W. Thatcher, A.A. Shah, Combust. Theory Modell. 7 (2003) 175–203.
[31] J.W. Dold, Combust. Theory Modell. 11 (2007) 909–948.
[32] V.V. Gubernov, H.S. Sidhu, G.N. Mercer, Combust. Theory Modell. 12 (2008) 407–431.
[33] G.J. Sharpe, Combust. Theory Modell. 12 (2008) 717–738.
[34] G.J. Sharpe, SIAM J. Appl. Math. 70 (2009) 866–884.
[35] V. Gubernov, A. Kolobov, A. Polezhaev, H. Sidhu, G. Mercer, Proc. R. Soc. A – Math. Phys. Eng. Sci. 466 (2010) 2747–2769.
[36] V.V. Gubernov, A.V. Kolobov, A.A. Polezhaev, H.S. Sidhu, Combust. Theory Modell. 15 (2011) 385–407.
[37] G.J. Sharpe, S.A.E.G. Falle, Combust. Flame 158 (2011) 925–934.
[38] H. Zhang, Z. Chen, Combust. Flame 158 (2011) 1520–1531.
[39] H. Zhang, P. Guo, Z. Chen, Proc. Combust. Inst. 34 (2013) 3267–3275.
[40] H. Zhang, P. Guo, Z. Chen, Combust. Sci. Technol. 185 (2013) 226–248.
[41] G. Joulin, P. Clavin, Combust. Flame 35 (1979) 139–153.
[42] C.K. Law, C.J. Sung, Prog. Energy Combust. Sci. 26 (2000) 459–505.
[43] Z. Chen, Y. Ju, Int. J. Heat Mass Transfer 51 (2008) 6118–6125.
[44] Z. Chen, X. Gou, Y. Ju, Combust. Sci. Technol. 182 (2010) 124–142.
[45] V.N. Kurdyumov, D. Fernandez-Galisteo, Combust. Flame 159 (2012) 3110–3118.
[46] Y. Saiki, Y. Suzuki, Proc. Combust. Inst. 34 (2013) 3395–3402.
[47] C.K. Law, Combustion Physics, Cambridge University Press, 2006.
[48] X. Wang, C.K. Law, J. Chem. Phys. 138 (2013) 134305.